ChemComm

Accepted Manuscript

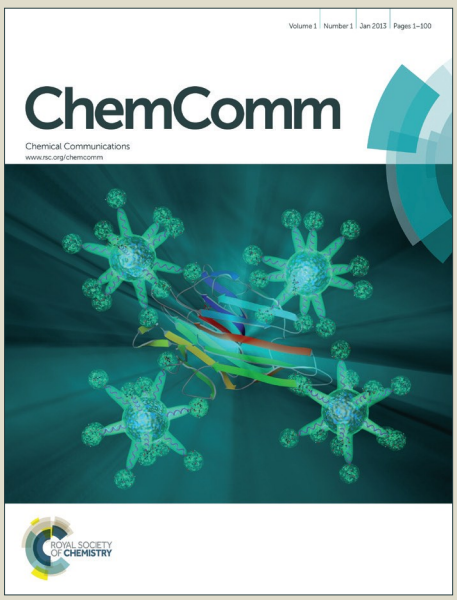

ROYAL SOCIETY OF CHEMISTRY

www.rsc.org/chemcomm

ChemComm

COMMUNICATION

The active site architecture in peroxiredoxins: a case study for *Mycobacterium tuberculosis* AhpE

Received 00th January 20xx,
Accepted 00th January 20xx

DOI: 10.1039/x0xx00000x

www.rsc.org/

Brandán Pedre[a,b,c] Laura A. H. van Bergen[b,c,d], Anna Palló[a,b,c], Leonardo A. Rosado[a,b,c], Veronica Tamu Dufe[a,b,c], Inge Van Molle[a,b,c], Khadija Wahni[a,b,c], Huriye Erdogan[a,b,c], Mercedes Alonso[d], Frank De Proft[d] and Joris Messens[a,b,c]

Peroxiredoxins catalyze the reduction of peroxides, a process of vital importance to survive oxidative stress. A nucleophilic cysteine, also known as the peroxidatic cysteine, is responsible for this catalytic process. We used the *Mycobacterium tuberculosis* alkyl hydroperoxide reductase E (MtAhpE) as a model to investigate the role of the chemical environment on the specificity of the reaction. Using an integrative structural (R116A - PDB 4XIH; F37G – PDB 5C04), kinetic and computational approach, we explain the mutational effects of key residues in its environment. This study shows that the active site residues are specifically oriented to create an environment which selectively favours a reaction with peroxides.

Peroxiredoxins (Prxs, EC 1.11.1.15) are ubiquitous peroxidases that broadly catalyze the reduction of peroxides such as hydrogen peroxide (H_2O_2) or organic hydroperoxides. They play a pivotal role in several physiological functions, such as inflammation or fat metabolism, and in different pathologies, such as cancer or neurological diseases[1-4]. The biological relevance of peroxiredoxins is due to their hub position in H_2O_2-mediated signaling, by establishing a H_2O_2 floodgate to redox-sensitive proteins or by redox transducing the oxidative signal, transferring the oxidizing equivalents to target proteins[5, 6].

The peroxide reduction occurs through the two-electron oxidation of the sulfur of a specialized cysteine residue, also known as the peroxidatic cysteine (C_P). This results in a cysteine sulfenic acid and an alkoxide or hydroxide leaving group:

$$\mathbf{Cys - S^- + ROOH \rightarrow Cys - SOH + RO^-}$$

The reaction rate is several orders of magnitude greater than that for free cysteine (10^3-10^7 $M^{-1}s^{-1}$). Along with their abundance (up to 1% of the proteome), this makes that Prxs are in the front line for H_2O_2 reduction[7]. However, despite the extensive research on the catalytic mechanism, the molecular factors that make these enzymes so efficient in reducing peroxides are not yet fully understood. Initially, H_2O_2 catalysis was associated with a low C_P thiol (-SH) pK_a, which assures thiolate ($-S^-$) presence at physiological pH. However, the deprotonation of the C_P thiol only contributes for a ten-fold increase in the H_2O_2 reduction rate when compared with free cysteine, leaving a 10^2 up to 10^6 difference of reactivity unaccounted for[8, 9]. In fact, cysteine is not essential for the binding of H_2O_2 to the peroxiredoxin active site, as shown in the crystal structure of a C_P to serine mutant in *Aeropyrum pernix* peroxiredoxin (PDB code 3A2W)[10]. Therefore, studies have focused on the conserved residues in the active site that are important for H_2O_2 binding and reduction, in particular the threonine from the PxxxTxxC sequence motif and an arginine distant in sequence but close to the active site. Understanding this conserved active site provides a potential target for structure-based drug design. The Prx crystal structures, including those ones complexed with H_2O_2 in the active site, suggest that the conserved arginine plays a pivotal role in bringing the oxygen of the peroxide closer to the C_P, weakening the O-O bond and stabilizing the transition state between the proximal O and the C_P[8, 10]. Mutations of the conserved arginine in Prxs lead to a significant drop in the peroxidatic activity[11, 12]. The structural data also suggest an important role of the threonine in the PxxxTxxC sequence motif[13], and dynamic and biochemical studies pointed out its relevance in, e.g. peroxide interaction, peroxide guidance to the active site, and activation of the C_P thiol [8, 10, 12].

In this work, we look at the structural and functional consequences of single point mutations within the Prx active site. We used *Mycobacterium tuberculosis* AhpE (MtAhpE) as a model because it has been extensively kinetically characterized, and upon H_2O_2 oxidation it changes its intrinsic fluorescence, which allows for single-turnover kinetic studies [14, 15]. Most of the Prxs contain a second cysteine which condensates with the cysteine sulfenic acid to form a disulfide bond (S-S), but AhpE is a single cysteine Prx, which makes the kinetic experiments less complex.

To evaluate the role of the residues in the C_P environment, we decided to mutate the conserved arginine 116 to an alanine (R116A), the conserved threonine 42 to a valine (T42V), and the phenylalanine localized N-terminally of the universally

[a] *Structural Biology Research Center, VIB, 1050 Brussels, Belgium*
[b] *Brussels Center for Redox Biology, 1050 Brussels, Belgium*
[c] *Structural Biology Brussels, Vrije Universiteit Brussel, 1050 Brussels, Belgium*
[d] *Research Group of General Chemistry, Vrije Universiteit Brussel, 1050 Brussels, Belgium*

† Footnotes relating to the title and/or authors should appear here.
Electronic Supplementary Information (ESI) available: [details of any supplementary information available should be included here]. See DOI: 10.1039/x0xx00000x

conserved PxxxTxxC sequence motif to a histidine (F37H), and analyzed the effects of these mutations on kinetics, structure and dynamics. The F37H mutation is inspired on the presence of a histidine at this position in other peroxiredoxins, such as the one from *A. pernix*[10]. In terms of H_2O_2 reduction rates, notable differences were observed. We compared the H_2O_2 consumption in function of time for wild type (WT), F37H, T42V and R116A MtAhpE, by following the ferrous oxidation of xylenol orange, a reagent used to determine H_2O_2 concentration in a solution mixture. We observed a clear impairment in H_2O_2 reduction for the R116A and T42V mutant, being T42V MtAhpE faster in H_2O_2 consumption than the R116A variant (Fig. 1). On the other hand, the F37H mutant shows no apparent impairment (Fig. 1). For determining the second-order rate constant of H_2O_2 reduction, we took advantage of the changes in intrinsic fluorescence upon protein oxidation: this method has been successfully performed for MtAhpE WT, resulting in a second-order rate constant of 8.2 X 10^4 M^{-1} s^{-1} at pH 7.4 and 25°C [14, 15]. For all mutants, we observed changes in intrinsic fluorescence proportional to the H_2O_2 concentration. At pH 7.4 and 25°C, a 10, 10^3 and 10^5-fold decrease was observed for F37H, T42V and R116A, respectively (Table 1). The decrease of the rate of the T42V and R116A MtAhpE is in line with what has been observed for other Prxs with mutations of the conserved active site threonine or arginine[11, 12, 16]. In order to assess whether the decrease in reactivity could be explained by a different deprotonation state of the C_P thiol, we measured the C_P pK_a of WT and the mutants. Unfortunately, we could not determine the C_P pK_a of T42V MtAhpE, as this mutant was not stable at a pH lower than 6.5. However, a similar mutation of the conserved Thr in Prdx5 (T44V) causes a C_P pK_a drop of approximately one unit, from 4.6 to 3.5[12]. Therefore, most likely the C_P pK_a of T42V MtAhpE will be lower than the one of WT MtAhpE. For the other MtAhpE variants, we observed that an increase of the cysteine pK_a does not account for a difference in reactivity, as shown from the pH-independent rate constants (Table 1). Therefore, the conserved arginine should play another important role for the reduction of H_2O_2, as the drop in k_{app} cannot be explained by C_P thiol deprotonation.

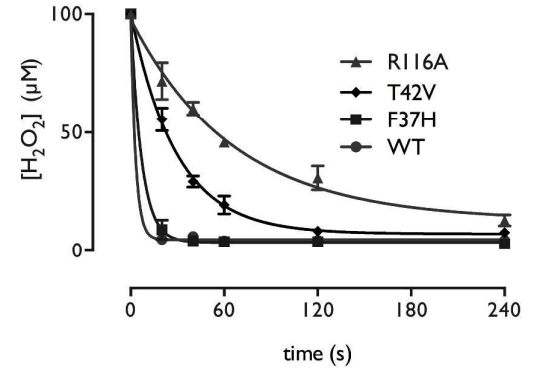

Fig. 1: H_2O_2 reduction by MtAhpE wild type (WT) and by its active site mutants. 100 µM H_2O_2 was added to an equimolar amount of MtAhpE, and the H_2O_2 concentration was followed in function of time (n=3).

Table 1: Kinetic parameters for the reduction of H_2O_2 by MtAhpE wild type (WT) and two active site mutants

Variant	k_{app} pH 7.4 (25°C)($M^{-1}s^{-1}$)	pK_a	% deprotonation C_P at pH 7.4	*k* (pH-independent)
WT	8.2 X $10^{4\,(13)}$	5.7 ± 0.1	98	8.36 X 10^4
F37H	(1.05 ± 0.04) X 10^3	5.9 ± 0.1	96.9	1.08 X 10^3
T42V	(5.77 ± 0.11) X 10^1	-	-	-
R116A	(7.11 ± 0.43) X 10^{-1}	6.4 ± 0.1	90.9	7.82 X 10^{-1}

To evaluate the consequences of these mutations on the architecture of the active site and the H-bonding network, we solved the X-ray crystal structures of the MtAhpE mutants (PDB code: 4XIH for R116A, 5C04 for F37H). It was not possible to obtain the crystal structure of the T42V variant, so we performed an *in silico* mutation on WT MtAhpE structure[17]. All variant structures were individually equilibrated in CHARMM in a 35 Å sphere of waters and subsequently analyzed with the non-covalent interaction (NCI) index method with the same procedure as described[17-19]. The NCI index has been proven to be better for determining H-bonds with sulfur atoms, and it quantifies the strength of the H-bond, which is is very useful to compare sulfur H-bonds in a different structural environment[17]. Comparing the mutant structures with the chain B from the WT MtAhpE crystal structure (PDB code: 4X0X[17]), no major changes were observed (root-mean-square deviation -RMSD- vs. WT structure is 0.220 Å for F37H, and 0.326 Å for R116A). Chain B was chosen because the orientation of R116 is similar to the orientation of the conserved arginine in other Prxs.

However, in the active site, several changes were observed in comparison with chain B of WT. The F37H mutation disrupts the active site architecture, and the hydrogen of the nitrogen in the imidazole group of H37 side chain acts as a H-bond donor which changes the orientation of the C_P, bringing it 1 Å closer to R116 (Fig. 2B). The side chain of the conserved threonine (T42) is also in a different position, it forms a hydrogen bond with the backbone oxygen of L39 and not with the C_P. In T42V MtAhpE, the C_P moves also closer to R116 (Fig. 2C). However, the underlying mechanism for this movement is different. Here, the absence of the hydroxyl group, which H-bonds with C_P, causes the C_P to re-orientate. In F37H MtAhpE, the C_P re-orientation is driven by its H-bonding with His instead of Thr. Calculations on small model systems showed that a H-bond in a Cys-His complex is 4 to 6 kcal/mol stronger than a H-bond in a Cys-Thr complex (see SI).

The presence and position of the conserved threonine is critical since it directs the peroxide into the active site, with the –OH group of its side chain acting as a H-bond acceptor, guiding the peroxide towards the C_P. This same threonine also increases the thiolate nucleophilicity upon peroxide binding and stabilizes the transition state[12]. In agreement with this observation, mutations of this threonine to valine in Prxs lead to a significant decrease of the H_2O_2 reduction rate[12, 16]. In the members of the Prx6 family, which effectively reduce H_2O_2 at a rate in the 10^7 $M^{-1}s^{-1}$ range, the histidine is located N-terminally of the PxxxTxxC sequence motif[20, 21]. However, the F37H replacement in MtAhpE decreases the rate of H_2O_2 reduction, as it disturbs the coordination between the C_P and the conserved threonine and arginine. On the other hand, the

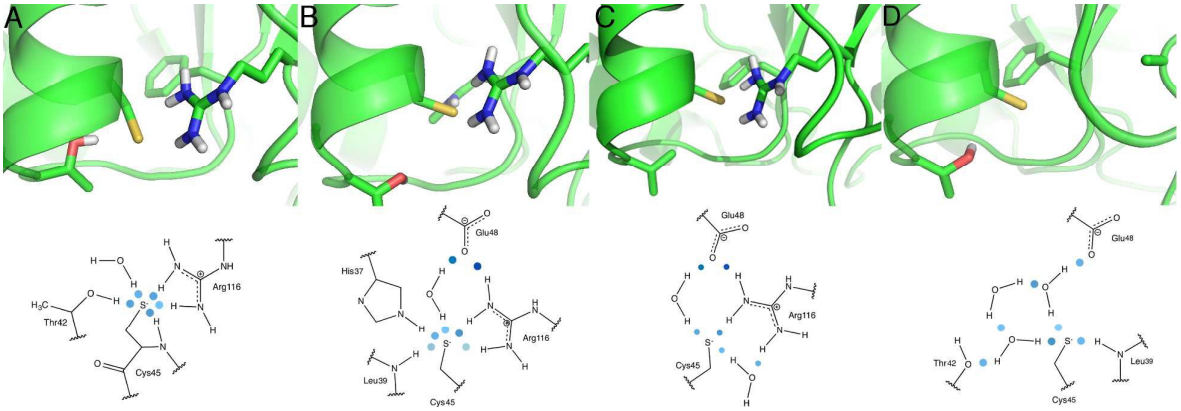

Fig. 2: Structure of the MtAhpE active site for WT (A), F37H (B), T42V (C) and R116A (D). The conserved cysteine, threonine and arginine residues are highlighted. Below each structure, the corresponding H-bonding network in the active site are shown. The color scheme next to the hydrogen bonds is based on the density measured by the NCI index: the darker the color, the stronger the bond.

R116A mutation leads to a surface-exposed C_P, which makes it more accessible for water molecules (Fig. 2D). Here, the orientation of the C_P sulfur is similar to the one of the F37H mutant, and the T42 side chain is not oriented towards the C_P, making H-bonding impossible. Instead, for both F37H and R116A mutants, the L39 amino group is H-bonding with the C_P (Fig. 2B and 2D). On the other hand, we do not observe H-bonding of L39 with the C_P in the T42V mutant (Fig. 2C).

The consequences of the F37H, T42V, and R116A mutations were also evaluated at the dynamic level. The crystal structures were taken as starting points for 30 ns molecular dynamics (MD) simulations, using a leap-frog algorithm. We calculated the average number of water molecules in the sphere surrounding the sulfur of the C_p. The simulations determined a considerable variation in the average number of water molecules in the active site area for each structure.

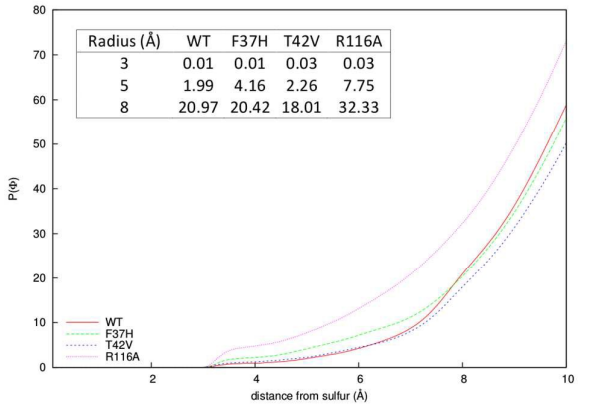

Fig. 3: Average number of water molecules (P(Φ)) around the sulfur atom of C_P in a sphere with a radius ranging from 0 to 10 Å, obtained from 30 ns molecular dynamics simulations. The insert shows the average for three different radii.

Within a sphere with a 5 Å radius surrounding the C_P, two water molecules are present in the WT structure, whereas more than 2 water molecules in T42V, 4 in F37H, and 8 in R116A were found (Fig. 3). Except for the T42V mutant, the number of water molecules inversely correlates to the second-order rate-constants with H_2O_2 (Fig. 3). This indicates that desolvation of the active site is critical for the reaction of the thiolate with H_2O_2, as the solvation shell must be disrupted to achieve the transition state. In fact, thiol disulfide exchange reactions are 10^3 faster in polar aprotic solvents (dimethylsulfoxide, dimethylformamide) than in water[22]. As more waters can enter the active site, also the possible positions of the peroxide in the active site will increase, and as a consequence the correct orientation for a nucleophilic attack will diminish, therefore decreasing the reaction rate.

Based on the H-bonding network of the R116A mutant, the solvation effect on the H_2O_2 reduction rate is evident (Fig. 2D). The arginine side chain is one of the bulkiest amino acid side chains, which effectively shields the cysteine from unwanted interactions with the solvent. As suggested from the *A. pernix* Prx crystal structure with H_2O_2 in its active site (PDB code 3A2V), the roles of the conserved arginine in the reaction are to activate the C_P as thiolate, to activate the oxygen atom of the incoming peroxide, and to position the peroxide closer to the C_P[8, 10]. However, we did not find any evidence for the interaction of H_2O_2 with R116. We used CHARMM to measure the H-bond lifetime of the residues in the WT structure when H_2O_2 is present, and despite applying constraints to the H_2O_2 to remain in the active site sphere, the MD-simulation determined that during the 30 ns simulation R116 is less than 5% of its time H-bonding with H_2O_2. Another study on Prdx5 is consistent with this finding, as the authors did not find interaction of the conserved arginine with H_2O_2 either[12]. This is in apparent contradiction to what has been described, although it might be possible that the arginine interaction with H_2O_2 is more important in the transition state[8, 15]. For the F37H mutant, we also observed an increase of the number of water molecules. That the active site of F37H is accessible to a higher number of water molecules is not immediately obvious from only counting the number of direct hydrogen bonds accepted

by the peroxidatic cysteine (Fig. 2B). Both the shifts in the position of T42 and the C_P are most likely the major cause of an increased number of water molecules in the active site, as the area between the T42 and the C_P becomes more solvent exposed (Fig. 2B). In agreement with this, the increase in C_P solvation has also been observed in the Prdx5 conserved threonine mutant, but was not further studied[12]. On the other hand, a discrete increase of the number of water molecules is observed in the T42V mutant. Why T42V MtAhpE loses its activity, despite the little increase in solvation, is probably due to the fundamental role of the threonine hydroxyl group in the peroxidation. For example, the *Leishmania donovani* tryparedoxin peroxidase loses most of its activity when the conserved threonine is mutated into a valine, but when the threonine is mutated into a serine, a 1.8-fold increase in peroxidatic activity is observed[16]. In fact, about 3% of the Prxs have a conserved serine instead of a threonine in their active site, indicating the importance of the hydroxyl group for the peroxidatic activity[23].

Our data indicate the importance of the conserved active site residues to exclude water, while orientating both C_P and H_2O_2 in the optimal position to react. Based on our calculations, structures, pK_a measurements, and kinetic data, we propose that the architecture of the active site, apart from its known functions, also prevents undesired interactions with water molecules.

Understanding the architecture of the active site microenvironment of Prxs forms the basis for unlocking the antioxidant properties of this family of enzymes. Furthermore, knowledge of the subtle interactions is important for the design of inhibitors. For example, a non-covalent inhibitor has recently been designed for the *Leishmania major* thioredoxin peroxidase[24]. As Prxs are potential therapeutic targets, these novel insights into the active site architecture will lead to better inhibitors for future treatments.

This work was financially supported from the following institutions: (i) agentschap voor Innovatie door Wetenschap en Technologie (IWT), (ii) Vlaams Instituut voor Biotechnologie (VIB), (iii) the SPR34 project of the Vrije Universiteit Brussel (VUB), Research Foundation Flanders (FWO) through research program G.0305.12, and (iv) Flanders Hercules Foundation (grant number HERC16) for the purification platform. We would also like to thank the infrastructure and staff from Soleil and Diamond synchrotrons for the X-ray data collection of the R116A and F37H crystals.

Notes and references

1. K. F. Bell and G. E. Hardingham, *Antioxidants & redox signaling*, 2011, **14**, 1467-1477.
2. H. M. Yun, K. R. Park, M. H. Park, D. H. Kim, M. R. Jo, J. Y. Kim, E. C. Kim, Y. Yoon do, S. B. Han and J. T. Hong, *Free radical biology & medicine*, 2015, **80**, 136-144.
3. B. Knoops, V. Argyropoulou, S. Becker, L. Ferte and O. Kuznetsova, *Molecules and cells*, 2016, DOI: 10.14348/molcells.2016.2341.
4. A. Perkins, L. B. Poole and P. A. Karplus, *Biochemistry*, 2014, **53**, 7693-7705.
5. M. C. Sobotta, W. Liou, S. Stocker, D. Talwar, M. Oehler, T. Ruppert, A. N. Scharf and T. P. Dick, *Nature chemical biology*, 2015, **11**, 64-70.
6. H. R. Latimer and E. A. Veal, *Molecules and cells*, 2016, DOI: 10.14348/molcells.2016.2327.
7. C. C. Winterbourn, *Nature chemical biology*, 2008, **4**, 278-286.
8. A. Hall, D. Parsonage, L. B. Poole and P. A. Karplus, *Journal of molecular biology*, 2010, **402**, 194-209.
9. G. Ferrer-Sueta, B. Manta, H. Botti, R. Radi, M. Trujillo and A. Denicola, *Chemical research in toxicology*, 2011, **24**, 434-450.
10. T. Nakamura, Y. Kado, T. Yamaguchi, H. Matsumura, K. Ishikawa and T. Inoue, *Journal of biochemistry*, 2010, **147**, 109-115.
11. P. Nagy, A. Karton, A. Betz, A. V. Peskin, P. Pace, R. J. O'Reilly, M. B. Hampton, L. Radom and C. C. Winterbourn, *J Biol Chem*, 2011, **286**, 18048-18055.
12. S. Portillo-Ledesma, F. Sardi, B. Manta, M. V. Tourn, A. Clippe, B. Knoops, B. Alvarez, E. L. Coitino and G. Ferrer-Sueta, *Biochemistry*, 2014, **53**, 6113-6125.
13. L. B. Poole and K. J. Nelson, *Molecules and cells*, 2016, **39**, 53-59.
14. M. Hugo, L. Turell, B. Manta, H. Botti, G. Monteiro, L. E. Netto, B. Alvarez, R. Radi and M. Trujillo, *Biochemistry*, 2009, **48**, 9416-9426.
15. A. Zeida, A. M. Reyes, M. C. Lebrero, R. Radi, M. Trujillo and D. A. Estrin, *Chemical communications*, 2014, **50**, 10070-10073.
16. L. Flohe, H. Budde, K. Bruns, H. Castro, J. Clos, B. Hofmann, S. Kansal-Kalavar, D. Krumme, U. Menge, K. Plank-Schumacher, H. Sztajer, J. Wissing, C. Wylegalla and H. J. Hecht, *Archives of biochemistry and biophysics*, 2002, **397**, 324-335.
17. L. van Bergen, M. Alonso, A. Pallo, L. Nilsson, F. De Proft and J. Messens, *Scientific reports*, 2016, **accepted**.
18. B. R. Brooks, C. L. Brooks, 3rd, A. D. Mackerell, Jr., L. Nilsson, R. J. Petrella, B. Roux, Y. Won, G. Archontis, C. Bartels, S. Boresch, A. Caflisch, L. Caves, Q. Cui, A. R. Dinner, M. Feig, S. Fischer, J. Gao, M. Hodoscek, W. Im, K. Kuczera, T. Lazaridis, J. Ma, V. Ovchinnikov, E. Paci, R. W. Pastor, C. B. Post, J. Z. Pu, M. Schaefer, B. Tidor, R. M. Venable, H. L. Woodcock, X. Wu, W. Yang, D. M. York and M. Karplus, *Journal of computational chemistry*, 2009, **30**, 1545-1614.
19. E. R. Johnson, S. Keinan, P. Mori-Sanchez, J. Contreras-Garcia, A. J. Cohen and W. T. Yang, *J Am Chem Soc*, 2010, **132**, 6498-6506.
20. K. J. Nelson, S. T. Knutson, L. Soito, C. Klomsiri, L. B. Poole and J. S. Fetrow, *Proteins*, 2011, **79**, 947-964.
21. J. C. Toledo, Jr., R. Audi, R. Ogusucu, G. Monteiro, L. E. Netto and O. Augusto, *Free radical biology & medicine*, 2011, **50**, 1032-1038.
22. R. Singh and G. M. Whitesides, *J Am Chem Soc*, 1990, **112**, 1190-1197.
23. A. Hall, K. Nelson, L. B. Poole and P. A. Karplus, *Antioxidants & redox signaling*, 2011, **15**, 795-815.
24. M. Brindisi, S. Brogi, N. Relitti, A. Vallone, S. Butini, S. Gemma, E. Novellino, G. Colotti, G. Angiulli, F. Di Chiaro, A. Fiorillo, A. Ilari and G. Campiani, *Scientific reports*, 2015, **5**, 9705.